



Dynamic triggering of earthquakes: the linear slip-dependent friction case

Christophe Voisin

► To cite this version:

Christophe Voisin. Dynamic triggering of earthquakes: the linear slip-dependent friction case. *Geophysical Research Letters*, 2001, 28 (17), pp.3357-3360. 10.1029/2001GL013101 . hal-00315344

HAL Id: hal-00315344

<https://hal.science/hal-00315344>

Submitted on 25 Jan 2021

HAL is a multi-disciplinary open access archive for the deposit and dissemination of scientific research documents, whether they are published or not. The documents may come from teaching and research institutions in France or abroad, or from public or private research centers.

L'archive ouverte pluridisciplinaire **HAL**, est destinée au dépôt et à la diffusion de documents scientifiques de niveau recherche, publiés ou non, émanant des établissements d'enseignement et de recherche français ou étrangers, des laboratoires publics ou privés.

Dynamic triggering of earthquakes: the linear slip-dependent friction case

Christophe Voisin¹

Laboratoire de Géophysique Interne et Tectonophysique, Observatoire de Grenoble
Université Joseph Fourier, Grenoble, France

Abstract. This paper is devoted to the modeling of dynamic triggering of earthquakes by a sinusoidal plane wave. I consider a 2D antiplane finite fault of length L under a linear slip-dependent friction law, characterized by a non-dimensional weakening parameter β . The finite fault is perturbed by an incident sinusoidal stress wave of wavelength λ and amplitude a . The positive pulse of the wave loads the fault and promotes the instability, while the negative pulse tends to heal the initiation process that may lead to the rupture. The occurrence of triggering depends on the balance between the loading terms and the intrinsic mechanics of the fault. Both amplitude and frequency exert a clock advance effect on the triggering. A threshold in frequency for the incident wave to trigger the rupture is revealed, which depends on the non-dimensional weakening parameter β and separates a nontriggering domain with stable slip from a triggering domain with unstable slip.

Introduction

The interaction between two faults is composed of a static part and of a dynamic part. During the last 30 years, many studies have developed the Coulomb stress method and used the static Coulomb Failure Stress, ΔCFS (see Harris [1998] and references therein). These studies most clearly demonstrate the correlation between the triggering of earthquakes and/or aftershocks and the positivity of the ΔCFS . However, it is clear that triggering also occurs in regions where $\Delta CFS \leq 0$, that is, in regions of stress shadows and also far away from the event, where static $\Delta CFS \approx 0$ as observed after the 1992 Landers earthquake (e.g., Hill *et al.* [1993]). The waves emitted during the mainshock seem to play a role in the spatial pattern of aftershocks and also on the remote seismicity [Kilb *et al.*, 2000]. Since rate-and-state friction laws are difficult to reconcile with this observation [Gomberg *et al.*, 1998], I investigate an alternative slip-dependent friction law [Ohnaka *et al.*, 1987]. In a recent study, Voisin *et al.* [2000] have shown the key role played by the dynamic stress pulse in the 23 November, 1980 Irpinia earthquake sequence. They have raised the possibility that dynamic stress waves could explain both aftershock triggering and long distance triggering of earthquakes, where the static stress field is insignificant. All over this paper, I focus on this last point. I consider a finite fault under slip-dependent friction that

is perturbed by a dynamic stress wave. I aim to test the ability of the incident stress wave to trigger the rupture on the fault, assuming that the static stress is zero.

Model

The finite fault

A 2D antiplane finite fault of length L embedded in an elastic space is considered. The fault length is set to $L = 10$ km, a typical value for a fault segment. The shear wave velocity is $c = 3000$ m/s, the density of the medium is $\rho = 3000$ kg/m³. The normal stress S_N is assumed to correspond to a depth of 5000 m.

The friction law

A linear slip-dependent friction law derived from the experimental works performed by Ohnaka *et al.* [1987] is implemented. The friction law is fully described by $\tau_s = \mu_s S_N$, $\tau_d = \mu_d S_N$, and D_c , respectively the static friction, the dynamic friction and the critical slip. I choose $\mu_s - \mu_d = 0.08$, which leads to a stress drop $\Delta\tau \approx 11.5$ MPa. The friction linearly decreases from τ_s to τ_d with the ongoing slip (initiation phase) until the slip reaches D_c on some part of the fault (Figure 1). The onset of rupture (and the occurrence of triggering) corresponds to the end of the initiation phase and to a propagation at the constant residual dynamic stress level. The initiation phase is characterized by the constant weakening rate α , given by the following relation:

$$\alpha = \frac{(\mu_s - \mu_d)S_N}{GD_c}, \quad (1)$$

where $G = \rho c^2$ is the rigidity modulus. Following Dascalu *et al.* [2000], I introduce the non-dimensional weakening parameter β as:

$$\beta = \alpha \times \frac{L}{2}, \quad (2)$$

where L is the fault length. This non-dimensional parameter completely characterizes the fault behavior. Dascalu *et al.* [2000] have performed a static stability analysis that reveals the intrinsic fault mechanics. They have computed the first nondimensional eigenvalue β_0 that determines the range of instability for the dynamic problem. This constant was found to be:

$$\beta_0 = 1.15777388 \dots \quad (3)$$

The fault behavior is governed by the relative magnitude of β and β_0 . In case of $\beta < \beta_0$, the fault is stable. In case of $\beta \geq \beta_0$, the fault is unstable and can be triggered. With the numerical values of the set of parameters, the previous condition of instability can be written as follows:

$$D_c < 1.9 \text{ m} \quad (4)$$

¹Now at Department of Geological Sciences, SDSU, San Diego, California.

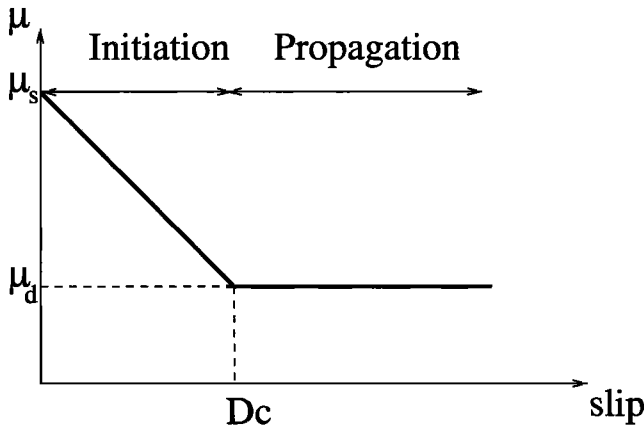


Figure 1. The linear slip-dependent friction law. The shear stress degrades from μ_s to μ_d with the ongoing slip until it reaches D_c , the critical slip. This is the initiation phase. At this point, the rupture propagates away on the fault.

State of stress

The state of stress on the fault and in the medium is homogeneous and equals the static friction level τ_s . This allows to focus only on the effect of the stress wave, and not on the possible effect of prestress.

The incident stress wave

The incident stress wave is a plane SH wave of sinusoidal shape. The wavelength λ and the amplitude a are both variable. The angle of incidence is set to $\theta = 45^\circ$.

Results

First case: $D_c = 1$ m (unstable fault)

Figure 2 presents the results of our computations with the following notations: the wave's amplitude a is normalized to the stress drop $\Delta\tau = \tau_s - \tau_d$ and the wavelength λ to the fault length L . Depending on the characteristics of the incident wave, the fault is triggered (crosses) or not (open squares). The limit between these two behaviors is formed by a vertical line, which proves that the wave's amplitude has not any effect on the occurrence of triggering under linear slip-dependent friction. The initiation duration is inversely proportional to both amplitude and wavelength, which both exert a clock advance effect. The main triggering factor is the wavelength λ , or reciprocally the wave's frequency $f = c/\lambda$. For this particular value of D_c and β , the limit between the triggering and the nontriggering domains is given for a ratio $\lambda/L = 0.39$, which gives $f_{lim} = 0.77$ Hz. Figure 3 presents the map view of the slip distribution in the two cases of nontriggering and triggering wave. When the wave's frequency $f > f_{lim}$ the incident wave does not trigger the rupture. The corresponding slip distribution is given by Figure 3a. The slip profile along the fault is not elliptical, but rather presents a directivity that is linked to the wave's propagation direction. The maximum of slip is correlated to the amplitude of the wave a . In the example shown in Figure 3a, this maximum is about 2.10^{-3} m. On the contrary, when $f < f_{lim}$ the incident stress wave triggers the rupture on the fault. Figure 3b shows the map view of the corresponding slip distribution. The slip profile along the fault is roughly elliptical (as expected for the development

of a shear crack). The maximum of slip has nothing more to do with the wave's amplitude a . It is rather controlled by the friction law and the fault length L .

Second case: $D_c = 2$ m (stable fault)

It is impossible to trigger the rupture on such a stable fault. The slip is necessary stable, aseismic. The slip distribution is extremely similar to the one observed in Figure 3a, corresponding to the nontriggering slip distribution of an unstable fault.

Dependence of f_{lim} with β

For a given value of L , and for each value of β such that $\beta > \beta_0$, it is possible to compute the corresponding value of f_{lim} that allows the triggering of rupture. Figure 4 presents the dependence of f_{lim} with the non-dimensional weakening parameter β . Globally, f_{lim} increases with β . Actually, the larger β is, the more unstable the fault is. Consequently, the limit frequency for the incident wave to trigger the rupture is larger, and the domain of triggering is extending towards higher frequencies. The results presented in Figure 4 are in perfect compliance with the static stability analysis performed by *Dasalu et al.* [2000]. As $\beta < \beta_0$, it is impossible to trigger the rupture and f_{lim} is not defined. As $\beta \geq \beta_0$, it is possible to define f_{lim} and to trigger the rupture, depending on the wave's characteristics. The noticeable point is the sudden increase in f_{lim} as $\beta \rightarrow \beta_1$, where β_1 is the second static eigenvalue obtained by *Dasalu et al.* [2000]. Actually the finite fault admits two deformation modes as $\beta \geq \beta_1$. The fault becomes far more unstable and this explains this sudden increase in the curve. The numerical investigation extends up to the third static eigenvalue. Unfortunately, because of discreteness of calculations, the jump in the curve is not as pronounced as the first one.

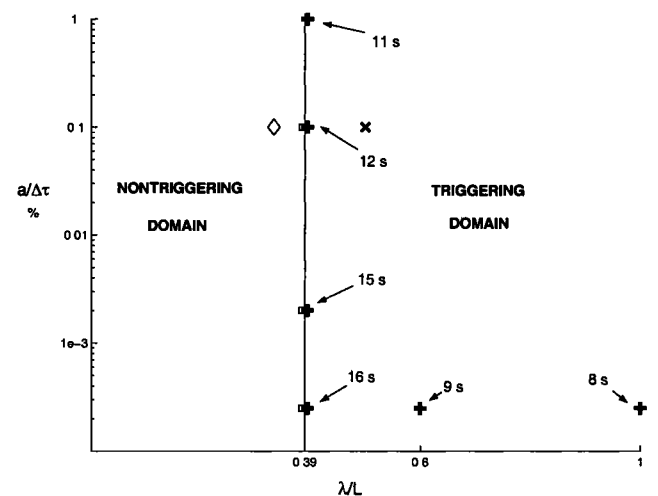


Figure 2. The normalized wave's amplitude versus the normalized wavelength. The critical slip is $D_c = 1$ m, the fault length $L = 10$ km. The transition between triggering (+) and nontriggering (□) is obtained for $\lambda/L = 0.39$. The time associated with the crosses correspond to the initiation duration before triggering. The amplitude has no effect on the limit, but exerts a clock-advance effect (as the wavelength does). The ◇ and the x denote the two cases presented in Figures 3a and 3b respectively. Note that the initiation duration may be much larger than the pulse duration that is here about 1.2 s at the triggering limit.

Interpretation

The results presented above can be physically understood if one think about the occurrence of triggering as the result of the balance between the intrinsic mechanics of the fault and the loading wave. When $\beta < \beta_0$ the fault is intrinsically stable and it is impossible to trigger the rupture. When $\beta \geq \beta_0$, the fault is intrinsically unstable. Therefore, the occurrence of triggering depends only on the loading characteristics. The positive pulse loads the fault and promotes the instability, while the negative pulse unloads the fault and tends to heal the rupture process by simply decreasing the stress on the fault. I have shown that only the wave's frequency may act on the occurrence of triggering. Let us make the following hypothesis: the duration of loading is important in the occurrence of triggering. The wave's frequency f is linked to the duration of loading on the fault by:

$$t_{load} = \frac{1}{f \sin \theta}, \quad (5)$$

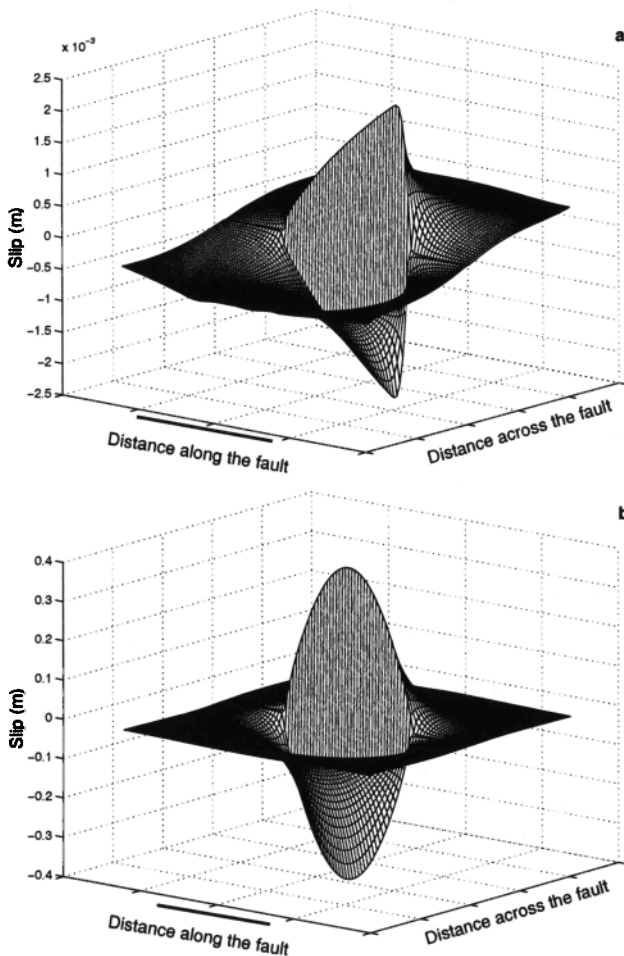


Figure 3. Map views of the slip distribution. Top: for a nontriggering case ($a/\Delta\tau = 0.1\%$, $\lambda/L = 0.333$). Note the asymmetry of the distribution and the small amplitude of slip on the fault. Bottom: for a triggering case ($a/\Delta\tau = 0.1\%$, $\lambda/L = 0.5$). The slip distribution is elliptical and the maximum of slip is large, controlled by D_c and the fault length L .

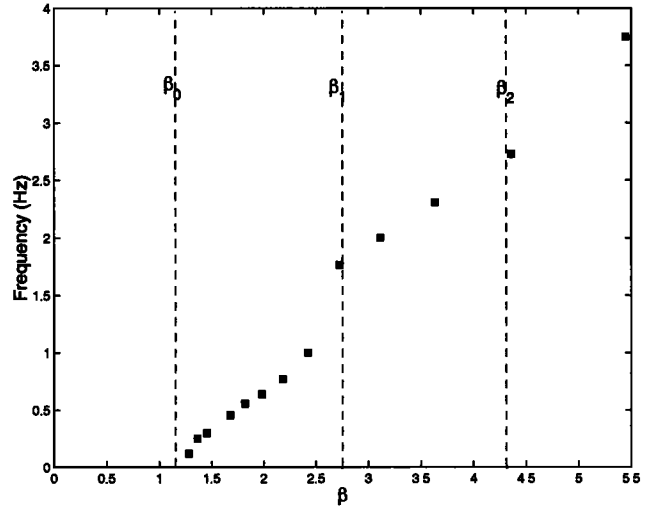


Figure 4. Limit frequency of triggering f_{lim} (for a fault length $L=10$ km) as a function of the non-dimensional weakening parameter β . The vertical dashed lines correspond to the static eigenvalues computed by *Dasalu et al.* [2000]. f_{lim} (black squares) is increasing with β , which indicates the increasing unstable behavior of the fault with β . The fault is perfectly stable and cannot be triggered as $\beta < \beta_0$. Note the sudden increase in f_{lim} as $\beta \rightarrow \beta_1$ which indicates the appearance of the second eigenmode of the fault. Because of discreteness of calculations, the second jump (as $\beta \rightarrow \beta_2$) is hardly noticeable.

where θ is the angle of incidence. *Dasalu et al.* [2000] have shown that the slip velocity on the fault grows as follows:

$$v \approx \exp(\lambda_0 t), \quad (6)$$

where λ_0 is the growth rate of the instability, prescribed by β . Consequently, for a given β , and for a given λ_0 , the slip velocity at the end of the loading increases with t_{load} . The initiation process is launched in such a way that inertial terms overcome the healing effect of the wave's negative pulse. This could explain why lower frequencies (associated with longer t_{load}) are able to trigger the rupture despite the negative pulse. This could explain also why the wave's amplitude a has no effect on the occurrence of triggering since the duration of loading does not depend on the wave's amplitude. But the main explanation is that a linear slip-dependent friction law is considered. The non-dimensional weakening parameter β is kept as a constant all along the friction law. Consequently λ_0 that is prescribed by β is also constant all along the law. Therefore, an increase in the wave's amplitude a implies an increase in the slip at the end of the loading, and not an increase in the slip velocity. This explains the clock advance effect of the wave's amplitude.

Discussion

The waves emitted during an earthquake seem to be able to trigger the seismicity at short or long distances, even in stress shadow zones. Numerous studies have also reported the occurrence of stable slip that was apparently triggered by the passage of waves [*Bodin et al.*, 1994]. *Bodin et al.* [1994] have shown that the stable slip triggered by the Landers rupture was delayed by a minute after the wave's passage and was going on for hours to weeks. However, stable slip is generally of small amplitude, about a few millimeters, and its duration is short. This extremely simple model

can't explain all the above mentioned observations. However, keeping in mind the assumptions I have done (simple shape of the wave, homogeneous stress field, linear friction), this model has shown that even for an unstable fault both stable and unstable slip could occur. A striking result is that a dynamic stress wave may trigger the delayed rupture of a fault under slip-dependent friction in the far field, where the static stress change is negligible. In the near field, both static and transient stresses have been shown to trigger earthquakes and aftershocks. Despite the difficulty to find any frequency threshold in the actual data, this simple model is consistent with the observation that low frequencies are more likely to trigger aftershocks and earthquakes [Anderson *et al.*, 1994]. In the linear friction case, the wave's amplitude exerts only a clock advance effect on the triggering. No intrinsic threshold in amplitude is observed. It would not be true under nonlinear friction, since both β and λ_0 would vary with the slip. Moreover, stress heterogeneities and understressed fault segments will presumably make the wave's amplitude as important as its frequency.

Acknowledgments. I would like to thank R. Harris, F. Cotton, and the two anonymous reviewers for their comments. This paper is dedicated to my father.

References

- Anderson, J.G., J.N. Brune, J.N. Louie, Y. Zeng, M. Savage, G. Yu, Q. Chen, and D. dePolo, Seismicity in the western Great Basin apparently triggered by the Landers, California, earthquake, 28 June 1998, *Bull. Seismol. Soc. Am.*, **84**, 863-891, 1994.
- Bodin, P., R. Bilham, J. Behr, J. Gomberg, and K.W. Hudnut, Slip triggered on southern California faults by the 1992 Joshua Tree, Landers and Big Bear earthquakes, *Bull. Seismol. Soc. Am.*, **84**, 806-816, 1994.
- Dascalu, C., I.R. Ionescu, and M. Campillo, Fault finiteness and initiation of dynamic shear instability, *Earth Planet. Sci. Lett.*, **177**, 163-176, 2000.
- Gomberg, J., N.M. Beeler, M.L. Blanpied, and P. Bodin, Earthquake triggering by transient and static deformations, *J. Geophys. Res.*, **103**, 24,411-24,436, 1998.
- Harris, R.A., Stress triggers, stress shadows, and implications for seismic hazard, *J. Geophys. Res.*, **103**, 24,347-24,358, 1998.
- Hill, D.P., P.A. Reasenberg, A. Michael, W.J. Arabaz, and G.C. Beroza, Seismicity remotely triggered by the magnitude 7.3 Landers, California, earthquake, *Science*, **260**, 1617-1623, 1993.
- Kilb, D., J. Gomberg, and P. Bodin, Triggering of aftershocks by dynamic stresses, *Nature*, **408**, 570-574, 2000.
- Ohnaka, M., Y. Kuwahara, and K. Yamamoto, Constitutive relations between dynamic physical parameters near a tip of the propagating slip zone during stick slip shear failure, *Tectonophysics*, **144**, 109-125, 1987.
- Voisin, C., M. Campillo, I.R. Ionescu, F. Cotton, and O. Scotti, Dynamic versus static stress triggering and friction parameters: Inferences from the November 23, 1980, Irpinia earthquake, *J. Geophys. Res.*, **105**, 21,647-21,559, 2000.

C. Voisin, Laboratoire de Géophysique Interne, Observatoire de Grenoble, Université Joseph Fourier, BP 53X, 38041 Grenoble Cedex, France. (cvoisin@obs.ujf-grenoble.fr)

(Received February 28, 2001; revised May 22, 2001; accepted June 27, 2001.)